

Accepted Manuscript

Synthesis, and docking studies of phenylpyrimidine-carboxamide derivatives bearing 1*H*-pyrrolo[2,3-*b*]pyridine moiety as c-Met inhibitors

Wufu Zhu, Wenhui Wang, Shan Xu, Jianqiang Wang, Qidong Tang, Chunjiang Wu, Yanfang Zhao, Pengwu Zheng

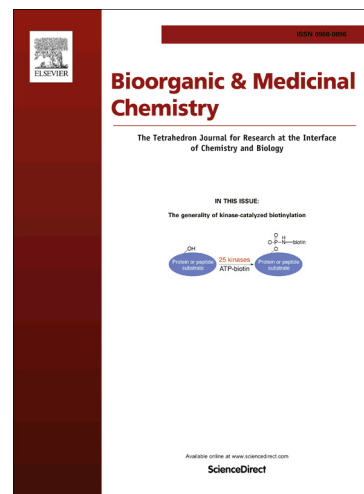
PII: S0968-0896(16)30136-5
DOI: <http://dx.doi.org/10.1016/j.bmc.2016.02.046>
Reference: BMC 12848

To appear in: *Bioorganic & Medicinal Chemistry*

Received Date: 10 February 2016
Revised Date: 27 February 2016
Accepted Date: 29 February 2016

Please cite this article as: Zhu, W., Wang, W., Xu, S., Wang, J., Tang, Q., Wu, C., Zhao, Y., Zheng, P., Synthesis, and docking studies of phenylpyrimidine-carboxamide derivatives bearing 1*H*-pyrrolo[2,3-*b*]pyridine moiety as c-Met inhibitors, *Bioorganic & Medicinal Chemistry* (2016), doi: <http://dx.doi.org/10.1016/j.bmc.2016.02.046>

This is a PDF file of an unedited manuscript that has been accepted for publication. As a service to our customers we are providing this early version of the manuscript. The manuscript will undergo copyediting, typesetting, and review of the resulting proof before it is published in its final form. Please note that during the production process errors may be discovered which could affect the content, and all legal disclaimers that apply to the journal pertain.



Synthesis, and docking studies of phenylpyrimidine-carboxamide derivatives bearing 1*H*-pyrrolo[2,3-*b*]pyridine moiety as c-Met inhibitors

Wufu Zhu^{1,†,*}, Wenhui Wang^{1,†}, Shan Xu^{1,†}, Jianqiang Wang², Qidong Tang¹, Chunjiang Wu¹, Yanfang Zhao³, Pengwu Zheng^{1*}

¹ School of Pharmacy, Jiangxi Science & Technology Normal University, Nanchang 330013, P. R. China.

² Fushun Center for Drug Control, Fushun, 113000, China;

³ Key Laboratory of Original New Drugs Design and Discovery of Ministry of Education, Shenyang Pharmaceutical University, 103 Wenhua Road, Shenhe District, Shenyang 110016, P. R. China.

*Correspondence author.

Tel/Fax: +86 791 8380-2393;

E-mail address: zhuwf@jxstnu.edu.cn, zhuwufu-1122@163.com (W. Zhu), zhengpw@126.com (P. Zheng).

Four series of phenylpyrimidine-carboxamide derivatives bearing 1*H*-pyrrolo[2,3-*b*]pyridine moiety (**14a–e**, **15a–g**, **16a–e** and **17a–g**) were designed, synthesized and evaluated for the IC₅₀ values against three cancer cell lines (A549, PC-3 and MCF-7). Four selected compounds (**15e**, **16a–b** and **17a**) were further evaluated for the activity against c-Met kinase, HepG2 and Hela cell lines. Most of the compounds showed excellent cytotoxicity activity and selectivity with the IC₅₀ valuables in single-digit μM to nanomole range. Eleven of them are equal to or more active than positive control Foretinib against one or more cell lines. The most promising compound **15e** showed superior activity to Foretinib against A549, PC-3 and MCF-7 cell lines, with the IC₅₀ values of 0.14±0.08 μM, 0.24±0.07 μM and 0.02±0.01 μM, which were 4.6, 1.6 and 473.5 times more active than Foretinib (0.64 ± 0.26 μM, 0.39 ± 0.11 μM, 9.47 ± 0.22 μM), respectively. Structure–activity relationships (SARs) and docking studies indicated that the replacement of phenylpicolinamide scaffold with phenylpyrimidine fragment of the target compounds was benefit for the activity. What's more, the introduction of fluoro atom to the aminophenoxy part played no significant impact on the activity and any substituent group on aryl group is unfavourable for the activity.

Key words: Phenylpyrimidine; 1*H*-Pyrrolo[2,3-*b*]pyridine; Synthesis; Docking; c-Met inhibitors; Antitumor activity

[†] These authors contribute equally to this work

*Corresponding author. Tel./fax: +86 791 83802393.

E-mail address: zhuwf@jxstnu.edu.cn, zhuwufu-1122@163.com (W. Zhu), zhengpw@126.com (P. Zheng).

1 Introduction

The c-Met receptor tyrosine kinase is aberrantly activated in many solid tumors. c-Met inhibitors may have therapeutic application in the treatment of various types of cancers. Cabozantinib^[1], a small molecule c-Met kinase inhibitor, was approved by FDA for the treatment of patients with progressive metastatic medullary thyroid cancer on November 29, 2012^[2]. In recent years, many derivatives of Cabozantinib were reported, such as Foretinib^[3], compounds I, II^[4-5]. The studies revealed that these compounds exhibited strong antitumor activity.

In our previous study, we reported a series of quinoline derivatives bearing phenylpicolinamide scaffold as potential c-Met inhibitors^[6]. In order to investigate the influence of the quinoline nucleus to the activity of target compounds, we kept the phenylpicolinamide scaffold unchanged and replaced the quinoline nucleus with 1*H*-pyrrolo[2,3-*b*]pyridine moiety to yield several series of new compounds^[7]. These 1*H*-pyrrolo[2,3-*b*]pyridine derivatives exhibited excellent antitumor activity. Structure–activity relationships (SARs) shown that the 1*H*-pyrrolo[2,3-*b*]pyridine scaffold benefit to the antitumor activity.

In this study, further modifications were carried out on these 1*H*-pyrrolo[2,3-*b*]pyridine derivatives. According to the theory of bioisosterism, we replaced the phenylpicolinamide scaffold with phenylpyrimidine moiety to get compounds **14a–e** and **15a–g**. What's more, fluoro atom was introduced to the aminophenoxy part of compounds **14a–e** and **15a–g** to study the effect to the activity and yielded **16a–e** and **17a–g**.

Herein we disclosed the synthesis and antitumor activity against A549, PC-3, MCF-7, Hela and HepG2 cancer cell lines, and c-Met kinase of phenylpyrimidine-carboxamide derivatives bearing 1*H*-pyrrolo[2,3-*b*]pyridine moiety. Moreover, docking studies were presented in this paper as well.

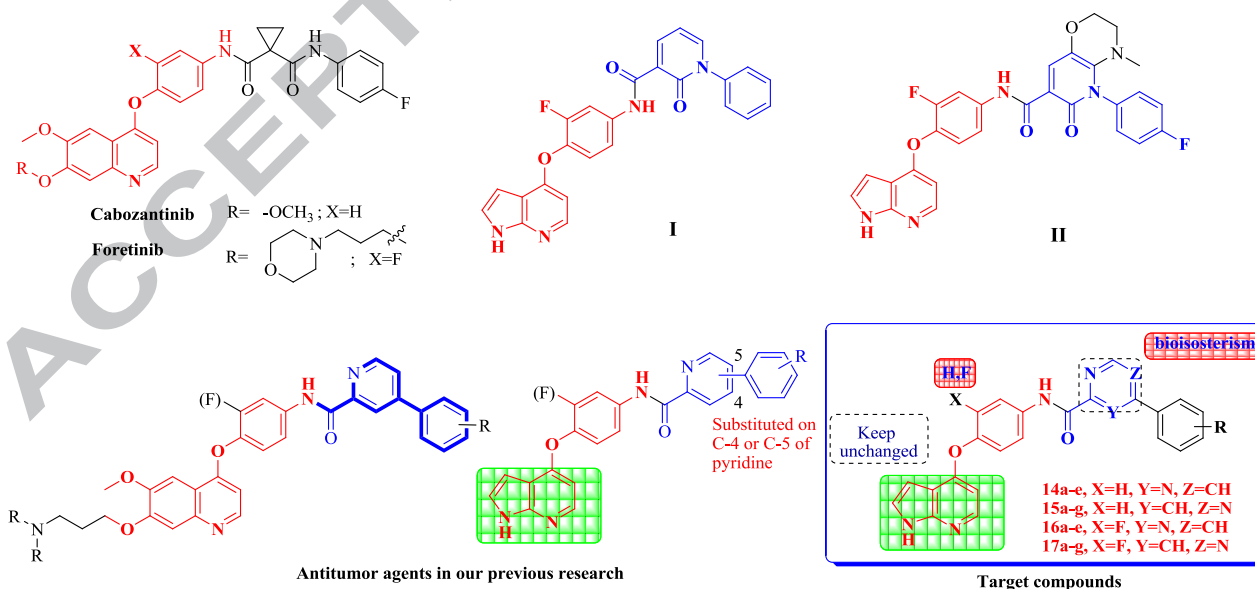


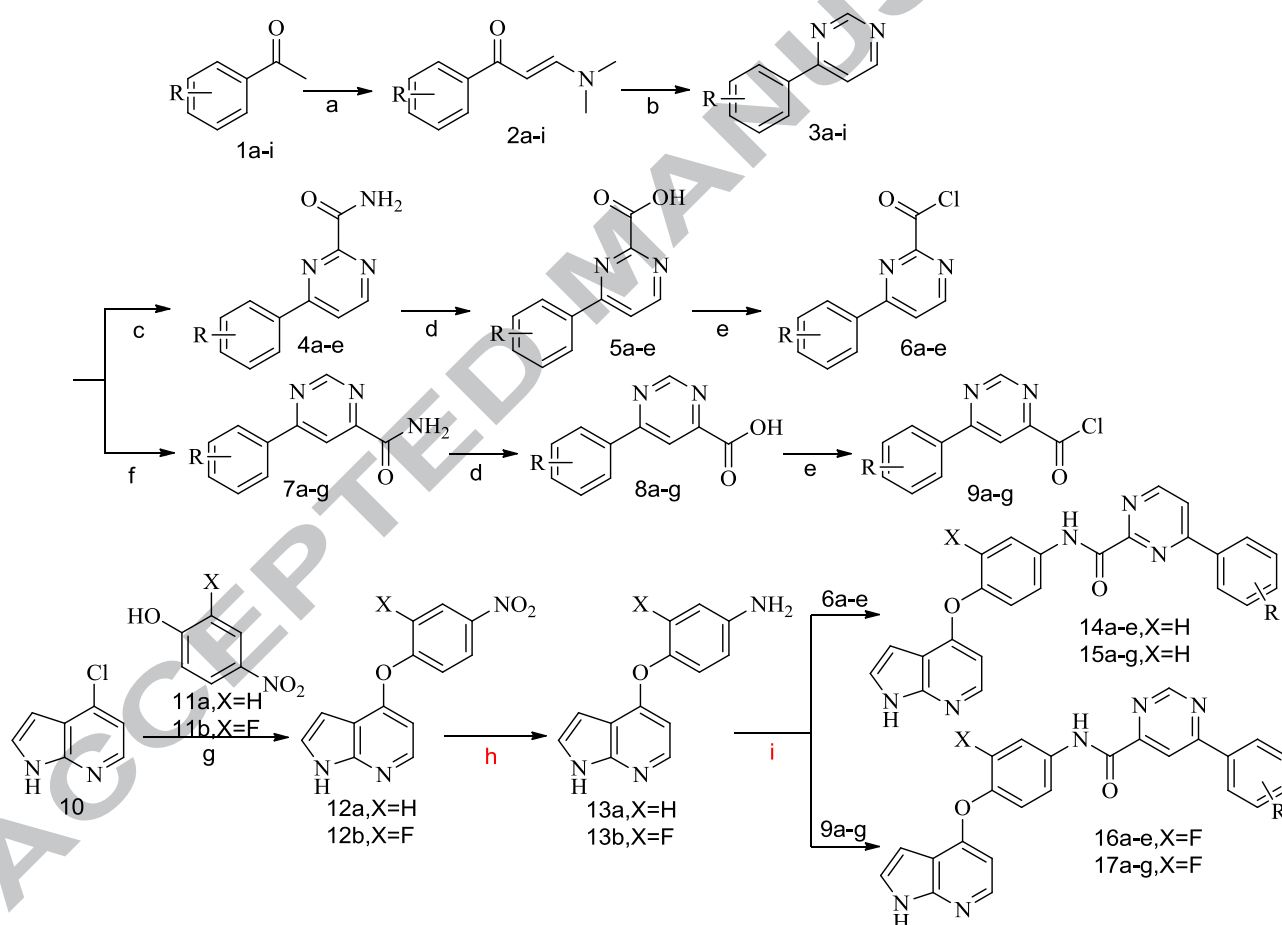
Fig. 1 Structures of small-molecule c-Met inhibitors and target compounds.

2. Chemistry

The preparation of target compounds **14a-e**, **15a-g**, **16a-e** and **17a-g** was described in Scheme 1.

The key intermediates 4-(4-aminophenoxy)-*N*-methylpicolinamide **13a,b** were achieved from 4-chloro-1*H*-pyrrolo[2,3-*b*]pyridine **10** via substitution reaction with 4-nitrophenol or 2-fluoro-4-nitrophenol **11a,b** and reduction with hydrazine hydrate in sequence as shown in Scheme 1.

Substituted 1-phenyl ethanone **1a-i** was reacted with *N,N*-Dimethylformamide dimethyl acetal (DMF-DMA) yielding compounds **2a-i**, which were then condensed with formamidine acetate to obtain compounds **3a-i**. Subsequently, compounds **3a-i** reacted with sulfuric acid and formamide with the absence of different catalyst to get **4a-e** and **7a-g**, respectively. Compounds **4a-e** and **7a-g** were hydrolyzed to corresponding carboxylic acid **5a-e** and **8a-g**, which were then chlorination with oxalyl chloride to obtain **6a-e** and **9a-g**, respectively. Finally, reaction of amides **13a,b** with phenylpyrimidine-carbonyl chloride **6a-e** or **9a-g** promoted by DIPEA in dichloromethane at room temperature yielded target compounds **14a-e**, **15a-g**, **16a-e** and **17a-g**, respectively.



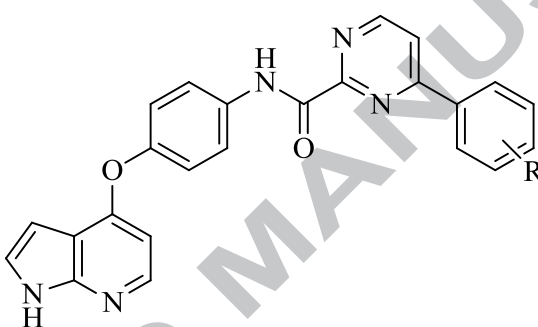
Scheme 1 Synthetic route of target compounds. Reagents and conditions: (a) DMF-DMA, 80°C, 8-12 h; (b) formamidine acetate, EtONa, EtOH, 70°C, 1h, reflux, 15-20 h; (c) acetamide, 98% H_2SO_4 , $\text{FeSO}_4 \cdot 7\text{H}_2\text{O}$, 30% H_2O_2 , 0-10°C, 1 h, 10-15°C, 30 min; (d) 20% H_2SO_4 , 100°C, 5-10 h; (e) SOCl_2 , reflux, 1h, CH_2Cl_2 , r.t., 0.5h; (f) acetamide, 98% H_2SO_4 , $\text{FeSO}_4 \cdot 7\text{H}_2\text{O}$, tert-Butyl hydroperoxide, 0-10°C, 1 h, 10-15°C, 30 min; (g) diphenyl ether, 190°C, 1 h; (h) $\text{N}_2\text{H}_4 \cdot \text{H}_2\text{O}$, FeCl_3 , activated carbon, EtOH, 10 min; (i) DIPEA, CH_2Cl_2 , r.t., 0.5h.

3. Results and discussion

3.1 Biological evaluation

Taking c-Met inhibitor Foretinib as reference compound, the target compounds (**14a–e**, **15a–g**, **16a–e** and **17a–g**) were evaluated for the cytotoxicity against three cancer cell lines A549 (human lung cancer), PC-3 (human prostatic cancer) and MCF-7 (human breast cancer) by 3-(4, 5-dimethylthiazolyl)-2, 5-diphenyltetrazolium bromide (MTT) cell proliferation assay. In addition, four selected compounds (**15e**, **16a–b** and **17a**) were evaluated for the IC_{50} values against HepG2, Hela cell lines and c-Met kinase *in vitro* by MTT assay or the Mobility shift assay with ATP concentration at K_m , together with reference compound Foretinib. The results expressed as IC_{50} values were summarized in Tables 1–5 and the values are the average of at least two independent experiments.

Table 1 Structures and cytotoxicity of compounds **14a–e**



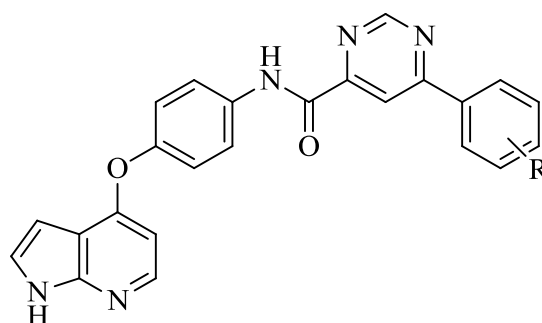
Compd. No.	R	IC_{50} (μM) ^a		
		A549	PC3	MCF-7
14a	4-CH ₃	2.38±1.10	6.14±1.01	6.41±1.00
14b	3-Cl	4.12±1.00	7.80±1.08	10.20±1.06
14c	4-OCH ₃	13.34±1.31	17.32±1.41	12.44±1.39
14d	4-Cl	22.38±1.15	NA ^c	NA
14e	4-F	NA	NA	NA
Foretinib ^b	-	0.64 ± 0.26	0.39 ± 0.11	9.47 ± 0.22

^a The values are an average of two separate determinations.

^b Used as a positive control

^c No Activity

Table 2 Structures and cytotoxicity of compounds **15a–g**



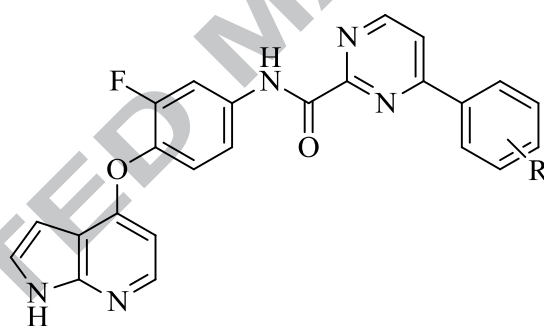
Compd. No.	R	IC ₅₀ (μM) ^a		
		A549	PC3	MCF-7
15a	4-OCH ₃	4.41±1.11	9.83±1.25	4.45±0.94
15b	4-F	12.99±0.92	NA ^c	15.86±0.97
15c	4-Cl	6.53±1.06	15.62±0.95	7.77±0.95
15d	4-CF ₃	9.38±1.02	2.16±1.64	6.24±1.12
15e	H	0.14±0.08	0.24±0.07	0.02±0.01
15f	4-Br	9.87±0.94	2.61±0.89	3.84±0.96
15g	4-CH ₃	5.41±1.00	9.88±1.19	1.62±0.78
Foretinib^b	-	0.64 ± 0.26	0.39 ± 0.11	9.47 ± 0.22

^a The values are an average of two separate determinations.

^b Used as a positive control

^c No Activity

Table 3 Structures and cytotoxicity of compounds **16a-e**



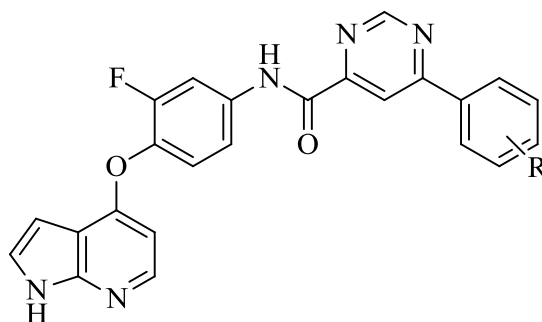
Compd. No.	R	IC ₅₀ (μM) ^a		
		A549	PC3	MCF-7
16a	4-CH ₃	1.15±0.14	0.52±0.12	7.17±1.02
16b	3-Cl	0.45±0.20	1.38±0.11	1.58±0.84
16c	4-NO ₂	4.47±1.21	12.14±1.08	NA ^c
16d	4-OCH ₃	15.43±1.23	14.08±1.44	8.96±1.51
16e	4-Cl	8.94±1.07	14.59±1.43	9.66±1.31
Foretinib^b	-	0.64 ± 0.26	0.39 ± 0.11	9.47 ± 0.22

^a The values are an average of two separate determinations.

^b Used as a positive control

^c No Activity

Table 4 Structures and cytotoxicity of compounds **17a-g**



Compd. No.	R	IC ₅₀ (μM) ^a		
		A549	PC3	MCF-7
17a	H	0.18±0.04	0.04±0.01	4.64±1.18
17b	4-OCH ₃	4.21±1.57	2.57±0.84	10.41±0.96
17c	4-F	14.24±0.66	NA ^c	NA
17d	4-Cl	3.36±0.14	3.20±1.33	26.94±1.62
17e	4-CF ₃	2.22±0.82	4.12±0.98	2.84±0.70
17f	4-Br	6.98±1.05	11.34±1.01	10.33±1.40
17g	4-CH ₃	8.60±0.67	24.92±0.68	6.73±0.83
Foretinib^b	-	0.64 ± 0.26	0.39 ± 0.11	9.47 ± 0.22

^a The values are an average of two separate determinations.

^b Used as a positive control

^c No Activity

Table 5 Cytotoxicity and c-Met kinase inhibitory activity of selected compounds **15e**, **16a**, **16b**, **17a**

Compd. No.	IC ₅₀ (μM) ^a		
	c-Met	Hela	HepG2
15e	0.12	0.40±0.15	3.11±0.75
16a	3.40	5.51±0.52	16.41±0.89
16b	2.20	3.35±0.49	9.34±0.64
17a	0.98	2.86±0.54	9.61±0.77
Foretinib^b	0.014	-	-

^a The values are an average of two separate determinations.

^b Used as a positive control

As shown in Tables 1–4, most of the four series of compounds showed excellent cytotoxicity activity against different cancer cells with potency from the single-digit μM to single-digit nanomole range. And the activity of the second, the third and the fourth series (**15a–g**, **16a–e** and **17a–g**) is much better than that of the first series (**14a–e**). Eleven of the target compounds showed better activity than positive control Foretinib against one or more cancer lines.

Among them, compounds **15e**, **16a–b** and **17a** showed superior activity to positive control Foretinib against all the three cancer cell lines. The most promising compound **15e** exhibit best activity against A549, PC-3 and MCF-7 cell lines with IC_{50} values of $0.14 \pm 0.08 \mu\text{M}$, $0.24 \pm 0.07 \mu\text{M}$ and $0.02 \pm 0.01 \mu\text{M}$, which were 4.6, 1.6 and 473.5 times more active than Foretinib ($0.64 \pm 0.26 \mu\text{M}$, $0.39 \pm 0.11 \mu\text{M}$, $9.47 \pm 0.22 \mu\text{M}$), respectively. The results suggested that the replacement of phenylpicolinamide scaffold with phenylpyrimidine fragment of the target compounds was benefit for the activity. What's more, the introduction of fluoro atoms to the aminophenoxy part played no significant impact on the activity.

Furthermore, different substitutions of aryl group affected the cytotoxicity of target compounds. It's seem to be that the presence of electron withdrawing group (-F, -Cl, -Br, -NO₂) at C-4 position decreased the activity of the target compounds, such as compounds **14d**, **14e**, **15b–d**, **15f**, **16c**, **16e**, **17c–d** and **17f**. However, the electron withdrawing group Cl atom at C-3 position is better than that at C-4 group. For example, the activity of compounds **14b**, **16b** is better than compounds **14d**, **16e**. In addition, compounds without substituent group on aryl group exhibit the best activity, such as compounds **15e**, **16a–b** and **17a**. The results suggest that any substituent group on aryl group is unfavourable for the activity.

Activity against c-Met kinase, Hela and HepG2 cell lines of compounds **15e**, **16a–b** and **17a** was further carried out in this paper to investigate the target and selectivity of these compounds. According to the results of Table 5, we can easily find that the four selected compounds showed moderate to excellent inhibitory on c-Met kinase, Hela and HepG2 cell lines. Compounds **15e** and **17a** are more active than that of compounds **16a–b**, especially compounds **15e** with IC_{50} value of $0.12 \mu\text{M}$ on c-Met kinase. The results prompt us that the compounds may be a series of c-Met kinase inhibitors.

3.2 Molecular docking study

To explore the binding modes of target compounds with the active site of c-Met, molecular docking simulation studies were carried out by using SURFLEX-DOCK module of SYBYL package version. Based on the *in vitro* inhibition results, we selected compound **15e**, our best c-Met inhibitor in this study, as the ligand example, and the structure of c-Met was selected as the docking model (PDB ID code : 3LQ8^[8]).

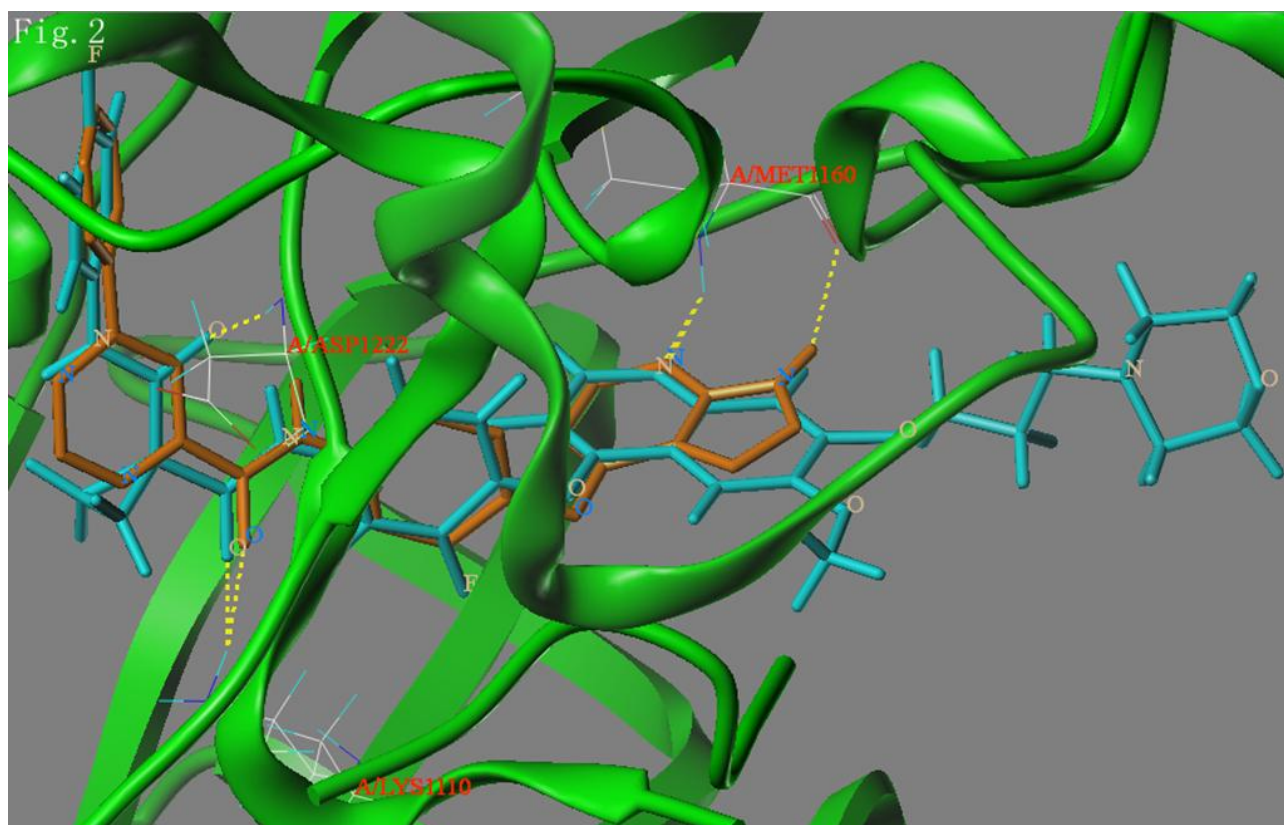


Fig. 2 Binding poses of compound **15e** with c-Met. The proteins were denoted by green ribbon. Compound **15e** and lead compound were denoted by orange and cyan sticks, respectively. H-bonding interactions between the **15e**, lead compound and c-Met were denoted by dashed lines in yellow.

The binding modes of compound **15e** and lead compound Foretinib were shown in Fig. 2. As depicted in Fig. 2, compound **15e** and lead compound can mostly overlap in the binding model and pyrrolo[2,3-*b*]pyridine nucleus, phenylpyrimidine-carboxamide moiety formed three hydrogen bonds with residues MET1160 and LYS1110, respectively. Analysis of compound **15e**'s binding mode in the active binding site demonstrated that the docking mode of the **15e** is similar to the lead compound with the same H-bond between pyrrolo[2,3-*b*]pyridine nucleus, phenylpyrimidine-carboxamide moiety and MET1160, LYS1110. The three hydrogen bonds really play an important role in increasing the inhibitory potency of pyrrolo[2,3-*b*]pyridine derivatives against c-Met kinase according to the docking results. Furthermore, the docking results also give us a new direction to design new c-Met inhibitors. The above-mentioned results of SARs analysis and molecular docking study may allow the rational design of more potent c-Met inhibitors.

4. Conclusions

In summary, we designed and synthesized four series of phenylpyrimidine-carboxamide derivatives bearing 1*H*-pyrrolo[2,3-*b*]pyridine nucleus and evaluated for the IC₅₀ values against three cancer cell lines and c-Met kinase. Eleven of them are equal to more active than positive control Foretinib against one or more cell lines. The most promising compound **15e** showed superior activity to Foretinib, with the IC₅₀ values of 0.14±0.08 μM, 0.24±0.07 μM and 0.02±0.01 μM, which were 4.6, 1.6 and 473.5 times more active than Foretinib (0.64 ± 0.26 μM, 0.39 ± 0.11 μM,

9.47 \pm 0.22 μ M), respectively. Structure–activity relationships (SARs) and docking studies indicated that the replacement of phenylpicolinamide scaffold with phenylpyrimidine fragment of the target compounds was benefit for the activity. What's more, the introduction of fluoro atom to the aminophenoxy part played no significant impact on the activity and any substituent group on aryl group is unfavourable for the activity. Further study will be carried out to identify the exact action mechanism in near future.

5. Experimental

5.1. Chemistry

All melting points were obtained on a Büchi Melting Point B-540 apparatus (Büchi Labortechnik, Flawil, Switzerland) and were 4 uncorrected. NMR spectra were performed using Bruker 400 MHz spectrometers (Bruker Bioscience, Billerica, MA, USA) with TMS as an internal standard. Mass spectra (MS) were taken in ESI mode on Agilent 1100 LCMS (Agilent, Palo Alto, CA, USA). All the materials were obtained from commercial suppliers and used without purification, unless otherwise specified. Yields were not optimized. TLC analysis was carried out on silica gel plates GF254 (Qindao Haiyang Chemical, China). All the materials were obtained from commercial suppliers and used without purification, unless otherwise specied. Yields were not optimized.

5.2 General procedure for the preparation of compounds **2a-i**.

The mixture of 1-phenyl ethanone (0.1mol) and DMF-DMA (39.8mL, 0.3mol) were heated to 80 °C, and monitored by TLC. Then the mixture was cooled to room temperature, poured into the mixture solution of petroleum ether and ether(120mL/40mL), and stirred 0.5 h. The precipitated solid was filtered off and dried to obtain the title compound **2a-i**.

5.3 Preparation of compounds **3a-i**.

Formamidine acetate(9.9 g, 0.096 mol) and sodium ethoxide(10.9 g, 0.16 mol) were dissolved in ethanol at 70 °C for 1 h. Then **2a-i** was added in the reaction solution slowly, refluxed for 15~20 h and monitored by TLC. The solution was concentrated in vacuum, the residue was resolved with dichloromethane (300 mL), washed with brine (60 mL), dried over anhydrous Na₂SO₄, and concentrated in vacuum to give the light yellow solids **3a-i**.

5.4 General procedure for the key intermediates **4a-e**.

The preparation of the key intermediates **4a-e** has been illustrated in detail in our previous work ^[6], and so the synthesis method would not be listed here.

5.5 General procedure for the key intermediates **7a-g**.

The preparation of the key intermediates **7a-g** was illustrated in Sakamoto's work^[9].

Concentrated sulfuric acid(20 mL) was added drop-wise to the mixture of **3a-i** (0.06 mol) and formamide(100mL) at 0-10°C. At the same time, 65% tert-butyl hydroperoxide(50 mL)and saturated FeSO₄·7H₂O (aq.100mL) were added drop-wise. The reaction solution was stirred at 10-15 °C for 0.5 h and then poured into water(2000 mL), basified with potassium hydroxide to pH 9, and extracted with dichloromethane (200 mL×3). The organic layer was dried over anhydrous Na₂SO₄, and concentrated in vacuum to obtain the title compound

7a-g.**5.6 General procedure for the preparation of 5a-e and 8a-g**

The mixture of an appropriate **4a-e** or **7a-g** (0.025 mol) and 20% H₂SO₄ (100 mL) was refluxed at 100°C for 5-10 h and monitored by TLC. The reaction mixture was poured into ice/water with stirring and filtered off and dried to obtain the desired target compounds **5a-e** or **8a-g**.

5.7 General procedure for the key intermediates 6a-e and 9a-g

The compounds **5a-e** or **8a-g** (0.02 mmol) were dissolved in thionyl chloride (8mL) and refluxed for 1 h. Then the reaction mixture was evaporated to yield the corresponding Chloride which were dissolved in dichloromethane (10mL). The solution was used for the next step without further purification.

5.8 . General procedure for the key intermediates 13a,b

The mixture of 4-chloro-1H-pyrrolo[2,3-*b*]pyridine (10 g, 66 mmol) and 4-nitrophenol **11a** (13.62 g, 98 mmol) or 2-fluoro-4-nitrophenol **11b** (15.56 g, 99 mmol) were refluxed in diphenyl ether at 190°C for 1 h and monitored by TLC. The mixture was cooled to 70 °C and poured into 400 mL ethyl acetate in an ice bath for 30 min, light yellow solid was precipitated, filtered off and dried to obtain the title compound **12a** or **12b**.

Then **12a** or **12b** (20 mmol) was refluxed with hydrazine hydrate (200 mmol), Ferric chlorid (10 mmol) and an appropriate amount of activated carbon in ethanol (100 mL)for 10min and monitored by TLC. The reaction solution was cooled. Then the insoluble was filtered, the filtrate was evaporated, after that water was added and stirred at room temperature for 30 min. Afterwards, the yellow solid was filtered off and dried to obtain the desired target compounds **13a** or **13b**.

5.9 General procedure for the preparation of target compounds 14a-e, 15a-g, 16a-e, 17a-g

A solution of phenylpyrimidine-carbonyl chloride **6a-e** or **9a-g** (0.82 mmol) in dichloromethane (10 mL) was added drop-wise to a solution of aniline **13a,b** (0.41 mmol) and diisopropylethylamine (0.49 mmol) in dichloromethane (10 mL) in an ice bath. Upon completion of the addition, the reaction mixture was removed from the ice bath and placed in room temperature for 30 min and monitored by TLC. The mixture was washed with 10% K₂CO₃ (50 mL ×3) followed by brine (50 mL ×1), and the organic phase was separated, dried, and evaporated to yield **14a-e**, **15a-g**, **16a-e** and **17a-g** which were recrystallized by isopropanol.

5.9.1 *N*-(4-((1*H*-pyrrolo[2,3-*b*]pyridin-4-yl)oxy)phenyl)-4-(*p*-tolyl)pyrimidine-2-carboxamide (14a)

Characters: light brown powder; Yield: 67.52%; ESI-MS *m/z*: [M+H]⁺422.5; m.p:234.9 ~ 239.6; ¹H NMR (400 MHz, DMSO) δ 11.73 (s, 1H), 10.98 (s, 1H), 9.43 (s, 1H), 8.58 (s, 1H), 8.24 (d, *J* = 7.9 Hz, 2H), 8.10 (d, *J* = 5.5 Hz, 1H), 8.04 (d, *J* = 8.4 Hz, 2H), 7.42 (d, *J* = 7.7 Hz, 2H), 7.38 – 7.30 (m, 1H), 7.25 (d, *J* = 8.4 Hz, 2H), 6.46 (d, *J* = 5.3 Hz, 1H), 6.23 (s, 1H), 2.42 (s, 3H).

5.9.2 *N*-(4-((1*H*-pyrrolo[2,3-*b*]pyridin-4-yl)oxy)phenyl)-4-(3-chlorophenyl)pyrimidine-2-carboxamide (14b)

Characters: light brown powder; Yield: 70.21%; ESI-MS *m/z*: [M+H]⁺442.9; m.p:243.1 ~ 247.8; ¹H NMR (400 MHz, DMSO) δ 11.64 (s, 1H), 10.90 (s, 1H), 9.39 (s, 1H), 8.57 (s, 1H), 8.26 (s, 1H), 8.19 (d, *J* = 7.4 Hz, 1H),

8.01 (d, $J = 4.9$ Hz, 1H), 7.94 (d, $J = 8.5$ Hz, 2H), 7.59 (d, $J = 7.8$ Hz, 1H), 7.52 (d, $J = 7.8$ Hz, 1H), 7.27 (s, 1H), 7.15 (d, $J = 8.4$ Hz, 2H), 6.36 (d, $J = 4.9$ Hz, 1H), 6.13 (s, 1H).

5.9.3 *N*-(4-((1*H*-pyrrolo[2,3-*b*]pyridin-4-yl)oxy)phenyl)-4-(4-methoxyphenyl)pyrimidine-2-carboxamide (**14c**)

Characters: light yellow powder; Yield: 67.14%; ESI-MS m/z : $[M+H]^+438.2$; m.p:201.3~204.5; 1H NMR (400 MHz, DMSO) δ 11.78 (s, 1H), 11.03 (s, 1H), 9.40 (s, 1H), 8.55 (s, 1H), 8.33 (d, $J = 8.9$ Hz, 2H), 8.10 (d, $J = 5.4$ Hz, 1H), 8.05 (d, $J = 8.9$ Hz, 2H), 7.39 – 7.36 (m, 1H), 7.25 (d, $J = 8.9$ Hz, 2H), 7.15 (d, $J = 8.9$ Hz, 2H), 6.44 (d, $J = 5.4$ Hz, 1H), 6.23 (s, 1H), 3.88 (s, 3H).

5.9.4 *N*-(4-((1*H*-pyrrolo[2,3-*b*]pyridin-4-yl)oxy)phenyl)-4-(4-chlorophenyl)pyrimidine-2-carboxamide (**14d**)

Characters: light yellow powder; Yield: 69.08%; ESI-MS m/z : $[M+H]^+442.9$; m.p:244.1~255.4; 1H NMR (400 MHz, DMSO) δ 11.78 (s, 1H), 11.08 (s, 1H), 9.48 (s, 1H), 8.64 (d, $J = 6.6$ Hz, 1H), 8.38 (d, $J = 8.4$ Hz, 2H), 8.09 (d, $J = 5.4$ Hz, 1H), 8.05 (d, $J = 8.8$ Hz, 2H), 7.68 (d, $J = 8.3$ Hz, 2H), 7.37 (s, 1H), 7.26 (d, $J = 8.7$ Hz, 2H), 6.44 (d, $J = 5.3$ Hz, 1H), 6.23 (s, 1H).

5.9.5 *N*-(4-((1*H*-pyrrolo[2,3-*b*]pyridin-4-yl)oxy)phenyl)-4-(4-fluorophenyl)pyrimidine-2-carboxamide (**14e**)

Characters: light brown powder; Yield: 66.98%; ESI-MS m/z : $[M+H]^+426.1$; m.p:184.2~186.8; 1H NMR (400 MHz, DMSO) δ 11.74 (s, 1H), 11.02 (s, 1H), 9.46 (s, 1H), 8.62 (s, 1H), 8.44 – 8.40 (m, 2H), 8.09 (d, $J = 5.4$ Hz, 1H), 8.04 (d, $J = 8.7$ Hz, 2H), 7.44 (t, $J = 8.8$ Hz, 2H), 7.36 (s, 1H), 7.24 (d, $J = 8.7$ Hz, 2H), 6.44 (d, $J = 5.3$ Hz, 1H), 6.22 (s, 1H).

5.9.6 *N*-(4-((1*H*-pyrrolo[2,3-*b*]pyridin-4-yl)oxy)phenyl)-6-(4-methoxyphenyl)pyrimidine-4-carboxamide (**15a**)

Characters: light yellow powder; Yield: 68.93%; ESI-MS m/z : $[M+H]^+438.5$; m.p:226.7 ~ 228.6; 1H NMR (400 MHz, DMSO) δ 11.73 (s, 1H), 10.97 (s, 1H), 9.40 (s, 1H), 8.58 (s, 1H), 8.36 (d, $J = 8.3$ Hz, 2H), 8.10 (d, $J = 4.6$ Hz, 1H), 8.04 (d, $J = 8.0$ Hz, 2H), 7.37 (s, 1H), 7.25 (d, $J = 8.2$ Hz, 2H), 7.15 (d, $J = 8.1$ Hz, 2H), 6.46 (d, $J = 4.5$ Hz, 1H), 6.23 (s, 1H), 3.88 (s, 3H).

5.9.7 *N*-(4-((1*H*-pyrrolo[2,3-*b*]pyridin-4-yl)oxy)phenyl)-6-(4-fluorophenyl)pyrimidine-4-carboxamide (**15b**)

Characters: light yellow powder; Yield: 67.42%; ESI-MS m/z : $[M+H]^+426.4$; m.p: 235.1 ~ 241.3; 1H NMR (400 MHz, DMSO) δ 11.74 (s, 1H), 11.00 (s, 1H), 9.46 (d, $J = 1.3$ Hz, 1H), 8.61 (dd, $J = 7.5, 1.3$ Hz, 1H), 8.45 – 8.40 (m, 2H), 8.09 (d, $J = 5.4$ Hz, 1H), 8.06 – 8.02 (m, 2H), 7.47 – 7.41 (m, 2H), 7.37 – 7.35 (m, 1H), 7.27 – 7.22 (m, 2H), 6.45 (d, $J = 5.4$ Hz, 1H), 6.22 (dd, $J = 3.4, 2.0$ Hz, 1H).

5.9.8 *N*-(4-((1*H*-pyrrolo[2,3-*b*]pyridin-4-yl)oxy)phenyl)-6-(4-chlorophenyl)pyrimidine-4-carboxamide (**15c**)

Characters: light yellow powder; Yield: 67.42%; ESI-MS m/z : $[M+H]^+442.9$; m.p: 271.1 ~ 277.4; 1H NMR (400 MHz, DMSO) δ 11.74 (s, 1H), 11.02 (s, 1H), 9.48 (d, $J = 1.3$ Hz, 1H), 8.63 (t, $J = 4.7$ Hz, 1H), 8.36 (dd, $J = 8.1,$

6.2 Hz, 2H), 8.09 (d, $J = 5.4$ Hz, 1H), 8.06 – 8.02 (m, 2H), 7.67 (dd, $J = 9.1, 2.3$ Hz, 2H), 7.38 – 7.34 (m, 1H), 7.27 – 7.22 (m, 2H), 6.45 (d, $J = 5.4$ Hz, 1H), 6.22 (dd, $J = 3.4, 2.0$ Hz, 1H).

5.9.9 *N*-(4-((1*H*-pyrrolo[2,3-*b*]pyridin-4-yl)oxy)phenyl)-6-(4-(trifluoromethyl)phenyl)pyrimidine-4-carboxamide (**15d**)

Characters: yellow powder; Yield: 69.02%; ESI-MS m/z : $[M+H]^+$ 476.4; m.p: 262.9 ~ 264.9; 1H NMR (400 MHz, DMSO) δ 11.74 (s, 1H), 11.06 (s, 1H), 9.55 (d, $J = 1.3$ Hz, 1H), 8.72 (d, $J = 1.3$ Hz, 1H), 8.55 (d, $J = 8.2$ Hz, 2H), 8.10 (d, $J = 5.4$ Hz, 1H), 8.07 – 8.02 (m, 2H), 7.97 (d, $J = 8.4$ Hz, 2H), 7.38 – 7.35 (m, 1H), 7.27 – 7.23 (m, 2H), 6.45 (d, $J = 5.4$ Hz, 1H), 6.22 (dd, $J = 3.4, 2.0$ Hz, 1H).

5.9.10 *N*-(4-((1*H*-pyrrolo[2,3-*b*]pyridin-4-yl)oxy)phenyl)-6-phenylpyrimidine-4-carboxamide (**15e**)

Characters: yellow powder; Yield: 67.77%; ESI-MS m/z : $[M+H]^+$ 408.4; m.p: 189.4~190.2; 1H NMR (400 MHz, DMSO) δ 11.74 (s, 1H), 11.02 (s, 1H), 9.48 (d, $J = 1.2$ Hz, 1H), 8.62 (d, $J = 1.2$ Hz, 1H), 8.34 (dd, $J = 7.5, 2.1$ Hz, 2H), 8.10 (d, $J = 5.4$ Hz, 1H), 8.07 – 8.02 (m, 2H), 7.65 – 7.59 (m, 3H), 7.38 – 7.34 (m, 1H), 7.25 (d, $J = 9.0$ Hz, 2H), 6.45 (d, $J = 5.4$ Hz, 1H), 6.22 (dd, $J = 3.4, 2.0$ Hz, 1H).

5.9.11 *N*-(4-((1*H*-pyrrolo[2,3-*b*]pyridin-4-yl)oxy)phenyl)-6-(4-bromophenyl)pyrimidine-4-carboxamide (**15f**)

Characters: yellow powder; Yield: 68.46%; ESI-MS m/z : $[M+H]^+$ 487.3; m.p: 263.1~266.3; 1H NMR (400 MHz, DMSO) δ 11.74 (s, 1H), 11.03 (s, 1H), 9.48 (s, 1H), 8.64 (s, 1H), 8.29 (d, $J = 8.4$ Hz, 2H), 8.09 (d, $J = 5.4$ Hz, 1H), 8.04 (d, $J = 8.8$ Hz, 2H), 7.81 (d, $J = 8.4$ Hz, 2H), 7.36 (s, 1H), 7.25 (d, $J = 8.8$ Hz, 2H), 6.44 (d, $J = 5.4$ Hz, 1H), 6.22 (s, 1H).

5.9.12 *N*-(4-((1*H*-pyrrolo[2,3-*b*]pyridin-4-yl)oxy)phenyl)-6-(*p*-tolyl)pyrimidine-4-carboxamide (**15g**)

Characters: yellow powder; Yield: 66.72%; ESI-MS m/z : $[M+H]^+$ 422.5; m.p: 239.6~244.2; 1H NMR (400 MHz, DMSO) δ 11.75 (s, 1H), 11.00 (s, 1H), 9.43 (s, 1H), 8.57 (s, 1H), 8.23 (d, $J = 8.0$ Hz, 2H), 8.09 (d, $J = 5.4$ Hz, 1H), 8.04 (d, $J = 8.8$ Hz, 2H), 7.41 (d, $J = 8.0$ Hz, 2H), 7.36 (s, 1H), 7.24 (d, $J = 8.8$ Hz, 2H), 6.44 (d, $J = 5.4$ Hz, 1H), 6.23 (s, 1H), 2.40 (s, 3H).

5.9.13 *N*-(4-((1*H*-pyrrolo[2,3-*b*]pyridin-4-yl)oxy)-3-fluorophenyl)-4-(*p*-tolyl)pyrimidine-2-carboxamide (**16a**)

Characters: khaki powder; Yield: 67.89%; ESI-MS m/z : $[M+H]^+$ 440.4; m.p: 228.0 ~ 233.9; 1H NMR (400 MHz, DMSO) δ 11.79 (s, 1H), 11.20 (s, 1H), 9.45 (s, 1H), 8.59 (s, 1H), 8.24 (d, $J = 7.8$ Hz, 2H), 8.18 – 8.11 (m, 1H), 8.10 (d, $J = 5.3$ Hz, 1H), 7.91 (d, $J = 8.6$ Hz, 1H), 7.50 – 7.43 (m, 2H), 7.41 – 7.37 (m, 2H), 6.42 (t, $J = 8.1$ Hz, 1H), 6.28 (s, 1H), 2.42 (s, 3H).

5.9.14 *N*-(4-((1*H*-pyrrolo[2,3-*b*]pyridin-4-yl)oxy)-3-fluorophenyl)-4-(3-chlorophenyl)pyrimidine-2-carboxamide (**16b**)

Characters: light green powder; Yield: 64.59%; ESI-MS m/z : $[M+H]^+$ 460.9; m.p.: 254.4 ~ 257.6; 1H NMR (400 MHz, DMSO) δ 11.78 (s, 1H), 11.23 (s, 1H), 9.51 (s, 1H), 8.69 (s, 1H), 8.38 (s, 1H), 8.32 (d, $J = 7.5$ Hz, 1H), 8.15 (s, 1H), 8.11 (d, $J = 7.0$ Hz, 1H), 7.91 (d, $J = 7.9$ Hz, 1H), 7.69 (s, 1H), 7.66 (d, $J = 7.7$ Hz, 1H), 7.45 (t, $J = 8.6$ Hz, 1H), 7.39 (s, 1H), 6.42 (s, 1H), 6.27 (s, 1H).

5.9.15 *N*-(4-((1*H*-pyrrolo[2,3-*b*]pyridin-4-yl)oxy)-3-fluorophenyl)-4-(4-nitrophenyl)pyrimidine-2-carboxamide (**16c**)

Characters: khaki powder; Yield: 63.47%; ESI-MS m/z : $[M+H]^+$ 471.4; m.p.: 288.5~290.4; 1H NMR (400 MHz, DMSO) δ 11.82 (s, 1H), 11.32 (s, 1H), 9.60 (s, 1H), 8.78 (s, 1H), 8.62 (d, $J = 7.6$ Hz, 3H), 8.44 (s, 3H), 8.10 (s, 1H), 7.47 (s, 1H), 7.40 (s, 1H), 6.41 (s, 1H), 6.28 (s, 1H).

5.9.16 *N*-(4-((1*H*-pyrrolo[2,3-*b*]pyridin-4-yl)oxy)-3-fluorophenyl)-4-(4-methoxyphenyl)pyrimidine-2-carboxamide (**16d**)

Characters: light yellow powder; Yield: 66.54%; ESI-MS m/z : $[M+H]^+$ 456.1; m.p.: 212.0~214.6; 1H NMR (400 MHz, DMSO) δ 11.84 (s, 1H), 11.23 (s, 1H), 9.40 (s, 1H), 8.55 (s, 1H), 8.33 (d, $J = 8.7$ Hz, 2H), 8.12 - 8.17 (m, 1H), 8.09 (d, $J = 5.4$ Hz, 1H), 7.91 (d, $J = 8.7$ Hz, 1H), 7.46 (t, $J = 9.1$ Hz, 1H), 7.40 (s, 1H), 7.14 (d, $J = 8.8$ Hz, 2H), 6.40 (d, $J = 5.4$ Hz, 1H), 6.28 (s, 1H), 3.86 (d, $J = 5.0$ Hz, 3H)

5.9.17 *N*-(4-((1*H*-pyrrolo[2,3-*b*]pyridin-4-yl)oxy)-3-fluorophenyl)-4-(4-chlorophenyl)pyrimidine-2-carboxamide (**16e**)

Characters: light yellow powder; Yield: 68.77%; ESI-MS m/z : $[M+H]^+$ 460.1; m.p.: 245.0~247.3; 1H NMR (400 MHz, DMSO) δ 11.83 (s, 1H), 11.29 (s, 1H), 9.50 (s, 1H), 8.66 (s, 1H), 8.38 (d, $J = 8.6$ Hz, 2H), 8.09 (d, $J = 5.4$ Hz, 1H), 7.92 (d, $J = 9.3$ Hz, 1H), 7.68 (d, $J = 8.5$ Hz, 2H), 7.47 (s, 1H), 7.41 - 7.39 (m, 1H), 6.40 (d, $J = 5.5$ Hz, 1H), 6.28 (d, $J = 2.0$ Hz, 1H), 5.77 (s, 1H).

5.9.18 *N*-(4-((1*H*-pyrrolo[2,3-*b*]pyridin-4-yl)oxy)-3-fluorophenyl)-6-phenylpyrimidine-4-carboxamide (**17a**)

Characters: light yellow powder; Yield: 68.61%; ESI-MS m/z : $[M+H]^+$ 426.4; m.p.: 226.8 ~ 228.9; 1H NMR (400 MHz, DMSO) δ 11.69 (s, 1H), 11.13 (s, 1H), 9.40 (s, 1H), 8.54 (s, 1H), 8.24 (s, 2H), 8.05 (d, $J = 5.2$ Hz, 1H), 8.00 (s, 1H), 7.82 (d, $J = 9.6$ Hz, 1H), 7.54 (s, 3H), 7.35 (t, $J = 8.9$ Hz, 1H), 7.30 (s, 1H), 6.32 (d, $J = 5.3$ Hz, 1H), 6.18 (s, 1H).

5.9.19 *N*-(4-((1*H*-pyrrolo[2,3-*b*]pyridin-4-yl)oxy)-3-fluorophenyl)-6-(4-methoxyphenyl)pyrimidine-4-carboxamide (**17b**)

Characters: light brown powder; Yield: 72.57%; ESI-MS m/z : $[M+H]^+$ 456.4; m.p.: 249.0 ~ 251.4; 1H NMR (400 MHz, DMSO) δ 11.78 (s, 1H), 11.17 (s, 1H), 9.41 (d, $J = 9.4$ Hz, 1H), 8.54 (s, 1H), 8.32 (d, $J = 8.2$ Hz, 2H), 8.12 - 8.16 (m, 2H), 7.90 (d, $J = 8.5$ Hz, 1H), 7.43 (t, $J = 9.1$, 1H), 7.37 (s, 1H), 7.15 (d, $J = 8.2$ Hz, 2H), 6.41 (d, $J =$

5.0 Hz, 1H), 6.28 (s, 1H), 3.91 (s, 3H).

5.9.20 *N*-(4-((1*H*-pyrrolo[2,3-*b*]pyridin-4-yl)oxy)-3-fluorophenyl)-6-(4-fluorophenyl)pyrimidine-4-carboxamide (**17c**)

Characters: white powder; Yield: 70.36%; ESI-MS *m/z*: [M+H]⁺444.4; m.p:269.8 ~ 274.1; ¹H NMR (400 MHz, DMSO) δ 11.79 (s, 1H), 11.23 (s, 1H), 9.48 (d, *J* = 1.3 Hz, 1H), 8.64 (d, *J* = 1.3 Hz, 1H), 8.45 – 8.40 (m, 2H), 8.12 – 8.16 (m, 1H), 8.09 (d, *J* = 5.4 Hz, 1H), 7.92 – 7.88 (m, 1H), 7.47 (t, *J* = 3.8 Hz, 1H), 7.45 (d, *J* = 3.4 Hz, 1H), 7.43 (d, *J* = 3.2 Hz, 1H), 7.40 – 7.37 (m, 1H), 6.41 (d, *J* = 5.4 Hz, 1H), 6.27 (dd, *J* = 3.4, 2.0 Hz, 1H).

5.9.21 *N*-(4-((1*H*-pyrrolo[2,3-*b*]pyridin-4-yl)oxy)-3-fluorophenyl)-6-(4-chlorophenyl)pyrimidine-4-carboxamide (**17d**)

Characters: light brown powder; Yield: 71.11%; ESI-MS *m/z*: [M+H]⁺460.9; m.p:256.4 ~ 265.9; ¹H NMR (400 MHz, DMSO) δ 11.79 (s, 1H), 11.23 (s, 1H), 9.49 (d, *J* = 1.3 Hz, 1H), 8.65 (d, *J* = 1.3 Hz, 1H), 8.40 – 8.35 (m, 2H), 8.12 – 8.16 (m, 1H), 8.09 (d, *J* = 5.4 Hz, 1H), 7.93 – 7.88 (m, 1H), 7.70 – 7.65 (m, 2H), 7.45 (t, *J* = 9.1 Hz, 1H), 7.40 – 7.37 (m, 1H), 6.41 (d, *J* = 5.4 Hz, 1H), 6.27 (dd, *J* = 3.4, 2.0 Hz, 1H).

5.9.22 *N*-(4-((1*H*-pyrrolo[2,3-*b*]pyridin-4-yl)oxy)-3-fluorophenyl)-6-(4-(trifluoromethyl)phenyl)pyrimidine-4-carboxamide (**17e**)

Characters: light brown crystals; Yield: 72.45%; ESI-MS *m/z*: [M+H]⁺494.4; m.p:264.5 ~ 278.3; ¹H NMR (400 MHz, DMSO) δ 11.79 (s, 1H), 11.27 (s, 1H), 9.56 (d, *J* = 1.3 Hz, 1H), 8.74 (d, *J* = 1.3 Hz, 1H), 8.56 (d, *J* = 8.2 Hz, 2H), 8.12 – 8.16 (m, 1H), 8.09 (d, *J* = 5.4 Hz, 1H), 7.98 (d, *J* = 8.3 Hz, 2H), 7.93 – 7.89 (m, 1H), 7.46 (t, *J* = 9.1 Hz, 1H), 7.41 – 7.37 (m, 1H), 6.41 (d, *J* = 5.4 Hz, 1H), 6.27 (dd, *J* = 3.4, 2.0 Hz, 1H).

5.9.23 *N*-(4-((1*H*-pyrrolo[2,3-*b*]pyridin-4-yl)oxy)-3-fluorophenyl)-6-(4-bromophenyl)pyrimidine-4-carboxamide (**17f**)

Characters: yellow powder; Yield: 71.70%; ESI-MS *m/z*: [M+H]⁺505.3; m.p:257.9~260.5; ¹H NMR (400 MHz, DMSO) δ 11.81 (s, 1H), 11.24 (s, 1H), 9.49 (s, 1H), 8.65 (s, 1H), 8.29 (d, *J* = 8.5 Hz, 2H), 8.12 – 8.16 (m, 1H), 8.09 (d, *J* = 5.5 Hz, 1H), 7.91 (d, *J* = 9.3 Hz, 1H), 7.81 (d, *J* = 8.5 Hz, 2H), 7.45 (t, *J* = 9.1 Hz, 1H), 7.40 (d, *J* = 2.3 Hz, 1H), 6.41 (d, *J* = 5.4 Hz, 1H), 6.28 (s, 1H).

5.9.24 *N*-(4-((1*H*-pyrrolo[2,3-*b*]pyridin-4-yl)oxy)-3-fluorophenyl)-6-(*p*-tolyl)pyrimidine-4-carboxamide (**17g**)

Characters: white powder; Yield: 71.67%; ESI-MS *m/z*: [M+H]⁺440.44; m.p: 250.4~251.9; ¹H NMR (400 MHz, DMSO) δ 11.79 (s, 1H), 11.21 (s, 1H), 9.44 (s, 1H), 8.58 (s, 1H), 8.24 (d, *J* = 8.1 Hz, 2H), 8.12 – 8.16 (m, 1H), 8.09 (d, *J* = 5.4 Hz, 1H), 7.90 (d, *J* = 8.9 Hz, 1H), 7.46 (d, *J* = 9.1 Hz, 1H), 7.43 (s, 1H), 7.41 (s, 1H), 7.39 (s, 1H), 6.40 (d, *J* = 5.4 Hz, 1H), 6.27 (s, 1H), 2.42 (s, 3H).

5. 10 Cytotoxicity assay in vitro

The cytotoxic activities of target compounds (**14a–e**, **15a–g**, **16a–e** and **17a–g**) were evaluated with A549, PC-3, MCF-7, HepG2 and Hela cell lines by the standard MTT assay *in vitro*, with compounds c-Met inhibitors Foretinib as positive control. The cancer cell lines were cultured in minimum essential medium (MEM) supplement with 10% fetal bovine serum (FBS). Approximately 4×10^3 cells, suspended in MEM medium, were plated onto each well of a 96-well plate and incubated in 5% CO₂ at 37°C for 24 h. The test compounds at indicated final concentrations were added to the culture medium and the cell cultures were continued for 72 h. Fresh MTT was added to each well at a terminal concentration of 5 µg/mL and incubated with cells at 37°C for 4 h. The formazan crystals were dissolved in 100 µL DMSO each well, and the absorbency at 492 nm (for absorbance of MTT formazan) and 630 nm (for the reference wavelength) was measured with the ELISA reader. All of the compounds were tested three times in each of the cell lines. The results expressed as inhibition rates or IC₅₀ (half-maximal inhibitory concentration) were the averages of two determinations and calculated by using the Bacus Laboratories Incorporated Slide Scanner (Bliss) software.

5. 11 *c-Met* kinase assay *in vitro*

The selected compounds (**15e**, **16a–b** and **17a**) are tested for their activity against c-Met kinase through the mobility shift assay [8-9]. All kinase assays were performed in 96-well plates in a 50 µL reaction volume. The kinase buffer contains 50 mM HEPES, pH 7.5, 10 mM MgCl₂, 0.0015% Brij-35 and 2 mM DTT. The stop buffer contains 100 mM HEPES, pH 7.5, 0.015% Brij-35, 0.2% Coating Reagent #3 and 50 mM EDTA. Dilute the compounds to 500 µM by 100% DMSO, then transfer 10 µL of compound to a new 96-well plate as the intermediate plate, add 90 µL kinase buffer to each well. Transfer 5 µL of each well of the intermediate plate to 384-well plates. The following amounts of enzyme and substrate were used per well: kinase base buffer, FAM-labeled peptide, ATP and enzyme solution. Wells containing the substrate, enzyme, DMSO without compound were used as DMSO control. Wells containing just the substrate without enzyme were used as low control. Incubate at room temperature for 10 min. Add 10 µL peptide solution to each well. Incubate at 28 °C for specified period of time and stop reaction by 25 µL stop buffer. At last collect data on Caliper program and convert conversion values to inhibition values. Percent inhibition = (max – conversion)/(max – min) × 100. “max” stands for DMSO control; “min” stands for low control.

5. 12 Docking studies

For docking purposes, the three-dimensional structure of the c-Met (PDB code: 3LQ8) were obtained from RCSB Protein Data Bank [4]. Hydrogen atoms were added to the structure allowing for appropriate ionization at physiological pH. The protonated state of several important residues, such as CYS919, and ASP1046 were adjusted by using SYBYL6.9.1 (Tripos, St. Louis, USA) in favor of forming reasonable hydrogen bond with the ligand. Molecular docking analysis was carried out by the SURFLEX-DOCK module of SYBYL 6.9.1 package to explore the binding model for the active site of c-Met with its ligand. All atoms located within the range of 5.0 Å from any atom of the cofactor were selected into the active site, and the corresponding amino acid residue was, therefore, involved into the active site if only one of its atoms was selected. Other default parameters were adopted in the SURFLEX-DOCK calculations. All calculations were performed on Silicon Graphics workstation.

Acknowledgments

We gratefully acknowledge the generous support provided by The National Natural Science Funds (81460527), Science and Technology Project Founded by the Education Department of Jiangxi Province (GJJ150796), Top-notch talent project of Jiangxi Science & Technology Normal University (2015QNBjRC001), Program of Key Laboratory of Drug Design and Optimization, Jiangxi Science & Technology Normal University (300098010306) and College Students' Science and Technology Innovation Project of Jiangxi Province (YC2015-X28).

References

- [1] You, W. K.; Sennino, B.; Williamson, C. W.; Falcón, B.; Hashizume, H.; Yao, L. C.; Aftab, D. T.; McDonald, D. M. *Cancer Res.* **2011**, *71*, 4758-4768.
- [2] <http://www.fda.gov/Drugs/InformationOnDrugs/ApprovedDrugs/ucm330213.htm> (U.S. Food and Drug Administration Updated: 11/30/2012, last accessed: 11/6/2015)
- [3] Qian, F.; Engst, S.; Yamaguchi, K.; Yu, P.; Won, K. A.; Mock, L.; Lou, T.; Tan, J.; Li, C.; Tam, D.; Loughheed, J.; Yakes, F. M.; Bentzien, F.; Xu, W.; Zaks, T.; Wooster, R.; Greshock, J.; Joly, A. H. *Cancer Res.* **2009**, *69*, 8009-8016.
- [4] Kim, K. S.; Zhang, L.; Schmidt, R.; Cai, Z. W.; Wei, D.; Williams, D. K.; Lombardo, L. J.; Trainor, G. L.; Xie, D.; Zhang, Y.; An, Y.; Sack, J. S.; Tokarski, J. S.; Darienzo, C.; Kamath, A.; Marathe, P.; Zhang, Y.; Lippy, J.; Jeyaseelan, R. Sr.; Wautlet, B.; Henley, B.; Gullo-Brown, J.; Manne, V.; Hunt, J. T.; Fargnoli, J.; Borzilleri, R. M. *J. Med. Chem.* **2008**, *51*, 5330-5341.
- [5] Cheng, J.; Qin, J.; Ye, B. U.S. Patent 2014026679, **2014**
- [6] Tang, Q.; Zhao, Y.; Du, X.; Gong, P.; Guo, C. *Euro. J. Med. Chem.* **2013**, *69*, 77-89.
- [7] Zhu, W.; Wang, W.; Xu, S.; Tang, Q.; Luo, R.; Wang, M.; Gong, P.; Zheng, P. *Bioorg. Med. Chem.* **2016**, *24*(4), 812-819.
- [8] Tang, Q.; Zhang, G.; Du, X.; Zhu, W.; Li, R.; Lin, H.; Li, P.; Cheng, M.; Gong, P.; Zhao, Y. *Bioorg. Med. Chem.* **2014**, *22*(4), 1236-1249.
- [9] Sakamoto, T. *Chem. Pharm. Bull.* **1980**, *28*(2), 571-577.
- [10] Wu, C.; Wang, M.; Tang, Q.; Luo, R.; Chen, L.; Zheng, P.; Zhu, W. *Molecules* **2015**, *20*, 19361-19371.
- [11] Zhu, W.; Liu, Y.; Zhai, X.; Wang, X.; Zhu, Y.; Wu, D.; Zhou, H.; Gong, P.; Zhao, Y. *Euro. J. Med. Chem.* **2012**, *57*, 162-175.

Legends

Fig. 1 Structures of small-molecule c-Met inhibitors and target compounds.

Fig. 2 Binding poses of compound **15e** with c-Met. The proteins were denoted by green ribbon. Compound **15e** and lead compound were denoted by orange and cyan sticks, respectively. H-bonding interactions between the **15e**, lead compound and c-Met were denoted by dashed lines in yellow.

Scheme 1 Synthetic route of target compounds.

Reagents and conditions: (a) DMF-DMA, 80°C, 8-12 h; (b) formamidine acetate, EtONa, EtOH, 70°C, 1h, reflux, 15-20 h; (c) acetamide, 98% H₂SO₄, FeSO₄·7H₂O, 30% H₂O₂, 0-10°C, 1 h, 10-15°C, 30 min; (d) 20% H₂SO₄, 100°C, 5-10 h; (e) SOCl₂, reflux, 1h, CH₂Cl₂, r.t., 0.5h; (f) acetamide, 98% H₂SO₄, FeSO₄·7H₂O, tert-Butyl hydroperoxide, 0-10°C, 1 h, 10-15°C, 30 min; (g) diphenyl ether, 190°C, 1 h; (h) N₂H₄·H₂O, FeCl₃, activated carbon, EtOH, 10 min; (i) DIPEA, CH₂Cl₂, r.t., 0.5h.

Table 1 Structures and cytotoxicity of compounds **14a-e**

^a The values are an average of two separate determinations.

^b Used as a positive control

^c No Activity

Table 2 Structures and cytotoxicity of compounds **15a-g**

^a The values are an average of two separate determinations.

^b Used as a positive control

^c No Activity

Table 3 Structures and cytotoxicity of compounds **16a-e**

^a The values are an average of two separate determinations.

^b Used as a positive control

^c No Activity

Table 4 Structures and cytotoxicity of compounds **17a-g**

^a The values are an average of two separate determinations.

^b Used as a positive control

Table 5 Cytotoxicity and c-Met kinase inhibitory activity of selected compounds **15e, 16a, 16b, 17a**

^a The values are an average of two separate determinations.

^b Used as a positive control

Graphical Abstract

